Spectral windowing with chirped magneto-optical Bragg gratings

Fredrik Jonsson

National Microelectronics Research Centre, Lee Maltings, Prospect Row, Cork, Ireland

Christos Flytzanis

Laboratoire Pierre Aigrain, Ecole Normale Superieure, F-75231 Paris, France, and Department of Physics, Chalmers University of Technology, S-41296 Gothenburg, Sweden

Received May 11, 2004; accepted August 5, 2004

We present a theory on a novel class of magneto-optical devices operated by means of magneto-optically induced refractive-index perturbations in chirped Bragg gratings. The predicted effect of the introduced perturbation is an opening of a narrow transmission window in the band-blocking transmission of the chirped grating. The narrow transmission window is tunable in wavelength, and relative transmission and the effects of multiple, spatially separated perturbations can also be superimposed, hence allowing for tunable, magneto-optically operated, multichannel add–drop multiplexors suitable for modularization in integrated optics.

OCIS codes: 130.3120, 230.3810, 230.5440, 050.2770.

1. INTRODUCTION

Magneto-optical Bragg gratings are dielectric media possessing a periodic or semiperiodic spatial modulation of their optical or magneto-optical properties along the direction of propagation of an optical wave. In this respect, we use the term "semiperiodic modulation" to mean a modulation with an adiabatically changing periodicity, in which case the resonance condition of the grating is changed along the grating. As a particular class of semiperiodic gratings, we in this paper address so-called chirped magneto-optical gratings, for which the grating period is a strictly decreasing or increasing function of the spatial coordinate.

The optical response of the grating can be either linear, in which case the material properties of the medium are independent of the optical field, or nonlinear, in which case the resonance peaks of the grating can be shifted dynamically by an intense optical beam. In particular, whenever nonlinear interactions are present in magneto-optic media with an optical feedback, such as in nonlinear magneto-optical cavities or gratings,[1] the resonance peaks for left and right circularly polarized modes will undergo a lifting of the degeneracy, and for intense optical beams magneto-optical mode locking and magneto-optically multistable devices employing the polarization state of the light as the controlling parameter have been devised.[1,2]

For the sake of simplicity, and for keeping the arguments to the basic physical principles of operation, we focus our attention in this paper on the application of chirped magneto-optical gratings in a linear optical domain. However, the device proposed in this work provides a basis for several promising features in a nonlinear optical domain as well, with the arguments as here outlined still valid in a nonlinear generalization.

Magneto-optical Bragg gratings composed of homogeneous layers of alternating optical and magneto-optical properties have recently gained considerable interest, and the fabrication of such devices has been reported by several groups.[3–6] For these devices mainly gallium gadolinium garnets and yttrium iron garnets have been used, owing to their reported high Verdet constants,[7–13] but semiconductors such as gallium arsenide have also recently gained some interest for magneto-optically tunable band properties of photonic crystals.[14]

In the case of optical Bragg gratings of a homogeneous period with a constant, nonmodulated Faraday effect superimposed over the grating, the only effect of the magneto-optical interaction is to shift the effective bias refractive index, with a different sign but an equal amplitude for left and right circularly polarized modes.[15] For this case, the Bragg resonance peaks of left and right circularly polarized light are shifted in opposite directions, introducing a polarization-state selectivity, with the resolution between the orthogonally polarized circular modes increasing with increasing grating strength and gyration constant. This mode of operation, with a homogeneous dc Faraday effect across the grating, is sometimes a convenient way of selecting a particular narrow-wavelength region, transmitting all other frequencies. In particular, this approach provides a separation between the reflection peaks, which is slightly tunable by means of varying the strength of an externally applied static magnetic field. In many cases, however, the desired mode of operation is rather to reflect a comparatively wide window of frequencies, for example of a certain wavelength band of operation of optical frequency channels, while allowing for the transmission of a single narrow band within the window. Here also a tunability of the transmitted channel within the full window is of some importance.

In this paper, we propose a novel class of devices, whose transmission characteristics are controlled by means of locally introduced magneto-optical perturbations of a chirped optical Bragg grating. It is shown that, for the proposed device, it is possible to achieve a broad spectral window of high reflection, while opening up this window to allow for the high transmission of certain narrow-wavelength intervals. The periodicity of the effective linear susceptibility of the medium can be achieved either by modulation of the all-optical (electric dipolar) properties (for example, through inscription of gratings in crystals by use of interference of short-wavelength optical radiation) or by means of a magneto-optical grating that is induced in the medium. The target application for this device is in magneto-optically operated tunable filters for optical add–drop multiplexing. The scalability of the device, introducing multiple spatially separated defects, is also discussed.

2. CHIRPED OPTICAL GRATINGS WITH MAGNETO-OPTICAL PERTURBATION

As in the case of all-optical Bragg gratings, the term "chirped" here originates from the acoustic analogy of a rising resonance frequency, here related to the spatially varying period of the grating, with the period either decreasing (negative chirp) or increasing (positive chirp) with an increasing coordinate along the direction of wave propagation.[16] In the terminology of magneto-optical Bragg gratings, there is a potential risk of confusion with the application of Bragg gratings to the sensing of a mechanical strain induced by a magnetic field strength; for this case, the resonance is all-optically achieved and is shifted only by means of a change of the all-optical modulation of the period and the refractive index.[17,18]

One way of inducing a periodic modulation, or equivalently a lattice of perturbations, of the magneto-optical effect along the propagation (for example, in an optical grating written by ultraviolet light exposure of doped silica) is the deposit of a coil of a conducting medium on top of the crystal. When a voltage difference is applied to the end electrodes, the current carried by the coil, via Ampères law, will induce a magnetic field directed along the waveguide, with its amplitude modulated around a zero median value. The coil can be fabricated down to sizes of the order of an optical wavelength by means of standard electron-beam lithographic processes in commercial polymeric resists, followed by metal deposition and development of the resist. The number of periods or perturbations can be arbitrary, down to a single current carrying a strip line; a schematic illustration of such a setup is shown in Fig. 1.

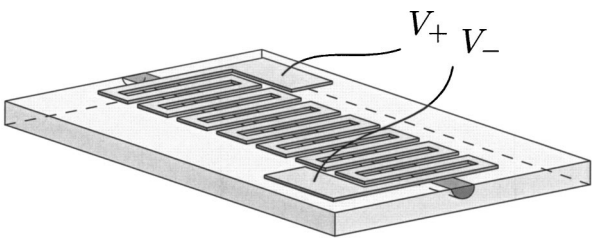

Fig. 1. Setup for generation of a magneto-optically induced lattice of perturbations, superimposed to an all-optical, electric-dipolar induced grating in a waveguide.

The refractive-index modulation of distributed Bragg gratings inscribed in silica is usually quite small,[16] typically of the order of $\Delta n \sim 10^{-3}$. Since this is nearly the same order as the refractive-index change that can be magneto-optically induced, with a differential shift between left and right circularly polarized modes, this allows for the interesting application of a magnetic field-induced shift of the optical resonances of an electric-dipolar, all-optical index modulation.

We start by considering the material properties of the electric-dipolar interaction, which in a linear optical domain here affects only the linear refractive index. In the following analysis, the refractive index is assumed to vary as

$$n(z) = n_0 + n_1 \sin[\theta(z)], \tag{1}$$

where n_0 is the bias of the refractive index, n_1 is half the peak-to-peak modulation depth, and $\theta(z)$ is the spatially varying phase function of the grating, here taken as

$$\theta(z) = (2\pi/\xi)\ln(1 + \xi z/\Lambda).$$

In this expression, ξ is the linear chirp parameter, and Λ is the initial spatial period of the grating. Notice that the phase function $\theta(z)$ will be a linear function of z only in the limit $\xi \to 0$, for which case $\theta(z) \to 2\pi z/\Lambda$.

Whenever the modulation depth n_1 is constant over the grating length, the projected local grating vector K_{loc} is from the index distribution in Eq. (1), given as

$$K_{\mathrm{loc}}(z) \equiv 2\pi/\Lambda_{\mathrm{loc}}(z) = \frac{\partial\theta(z)}{\partial z},$$

and when this differential is evaluated, the local period Λ_{loc} of the grating simply becomes the linear function

$$\Lambda_{\mathrm{loc}}(z) = \Lambda + \xi z.$$

From this the local resonant vacuum wavelength at which peak reflectance occurs is $\lambda_{\mathrm{res}}(z) = 2n_0\Lambda_{\mathrm{loc}}(z)$ in the absence of any static magnetic fields. For a grating of length L, the chirp parameter can hence be expressed in terms of the end resonance vacuum wavelengths of the grating as $\xi = (\lambda_b - \lambda_a)/(2n_0L)$.

In addition to the distribution [Eq. (1)] of the refractive index, the magneto-optical contribution provides the effective refractive indices of the medium for forward traveling left and right circularly polarized modes as

$$n_\pm = n(z) \pm g(z),$$

respectively, where for a magneto-optically homogeneous medium the spatially varying gyration constant is given as[19]

$$g(z) = i\chi_{xyz}^{(\mathrm{eem})}B_0(z)/2n_0.$$

where $\chi_{xyz}^{(\mathrm{eem})}$ is the linear magneto-optical susceptibility of the medium, in the molecularly nonresonant regime acting as a purely imaginary quantity,[20] and $B_0(z)$ is the static magnetic field, externally applied in the Faraday configuration.[21] Here the spatial variation of the gyration constant is assumed, without any loss of generality originated from a spatially varying magnetic field $B_0(z)$. However, the variation may equivalently arise from a spatially varying magneto-optical susceptibility.

Although optical gratings with chirped modulation have been extensively studied, we are here concerned

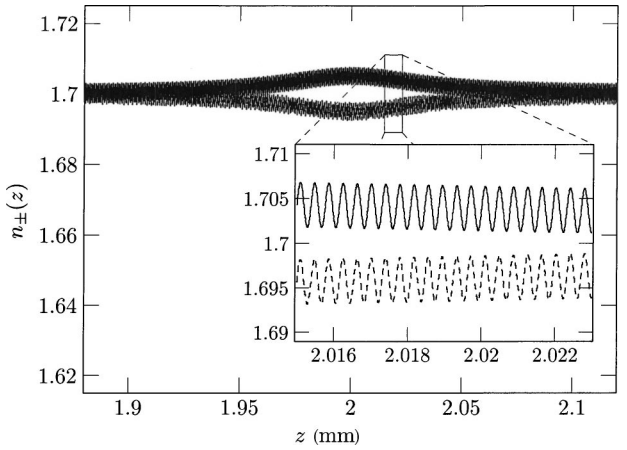

Fig. 2. Close-up figure of the distributions of effective refractive indices $n_+(z)$ and $n_-(z)$ experienced by forward-propagating left and right circularly polarized light (solid and dashed curves), respectively, in the region of the magneto-optically induced Lorentzian perturbation $g(z)$. For backward-traveling components of the wave, the situation becomes the opposite, with left and right polarized light instead experiencing the effective indices $n_-(z)$ and $n_+(z)$, respectively.

with analysis of the impact of the magneto-optically induced perturbations $g(z)$ on the transmission characteristics of such gratings. In particular, for the perturbing distribution of the magneto-optical gyration constant, we have chosen to analyze the Lorentzian function

$$g(z) = \frac{g_p}{1 + 4(z - z_p)^2/{w_p}^2},$$

where z_p is the spatial center position, g_p is the zero-to-peak amplitude at this center, and w_p is the half maximum full width of the perturbation. This perturbation corresponds exactly to the functional form of the magnetic field amplitude arising from a current carried by a wire oriented orthogonally to the direction of propagation of the light. The principal effective refractive-index profiles $n_+(z)$ and $n_-(z)$ of the perturbed grating, as experienced by forward-propagating left and right circularly polarized modes, respectively, are shown in Fig. 2.

3. NUMERICAL MODEL

As a design example for the magneto-optical grating, we consider in the absence of static magnetic fields a passband reflection filter ranging from vacuum wavelength $\lambda_a = 1300\,\text{nm}$ to $\lambda_b = 1320\,\text{nm}$, in which region we wish to open a transmission peak by magneto-optical means. For the bias refractive index, we assume $n_0 = 1.7$, which from the above relation between resonance wavelength λ_{res} and local grating period Λ_{loc} (assuming a positive chirp parameter $\xi > 0$) yields $\Lambda = 382.4\,\text{nm}$ for the grating period at the beginning of the grating. For a grating of length $L = 4.0\,\text{mm}$, the desired chirp parameter becomes $\xi = (\lambda_b - \lambda_a)/(2n_0L) = 1.47 \times 10^{-6}$. The intensity transmission I_{tr}/I_{in} of this grating in the absence of any static magnetic fields is shown in Fig. 3.

The transmission spectra throughout were calculated with a magneto-optically extended transfer matrix formulation of the electromagnetic wave propagation inside the grating, as described in more detail elsewhere.[19] Here we will outline only the basic assumptions used in the simulations. Essentially, the algorithm of the calculation relies on a discretized model of the continuous profile of the grating, as M thin slices of homogeneous media, for which analytical solutions exist. The general analytical solutions inside each homogeneous layer are subject to the boundary conditions of the interfacing layers, and by applying the requirement that the TE and TM components by electromagnetic conservation laws must be continuous across all interfaces,[21] one obtains a system of algebraic equations for the global, complex-valued transfer matrix of the grating. In formulating the boundary conditions, we have also taken into account the effect of a spatially varying gyration constant. Usually at interfaces the effect of this is very small in comparison with the effect due to the refractive-index contrast, but for large gratings the accumulated effect of a spatially varying gyration constant can be considerable.

In all simulations reported here, the spatial profile of the grating was sampled to $M = 4.0 \times 10^5$ homogeneous slices in order to properly resolve the periodicity of the grating, corresponding to an approximately 39 samples per spatial period. This oversampling is similar to the one used in, for example, direct scattering schemes for the calculation of the transmission properties of fiber Bragg gratings.[22]

The obtained solutions for the electromagnetic field are expressed in terms of the incident and transmitted intensities

$$I_{in} = (\epsilon_0 c/2)(|\mathbf{E}_\omega^+|^2 + |\mathbf{E}_\omega^-|^2)_{z=0},$$

$$I_{tr} = (\epsilon_0 c/2)(|\mathbf{E}_\omega^+|^2 + |\mathbf{E}_\omega^-|^2)_{z=L},$$

where $\mathbf{E}_\omega^+$ and $\mathbf{E}_\omega^-$ denote the forward-traveling left and right circularly polarized electrical field components of the optical wave, respectively, and the corresponding normalized ellipticities of the incident and transmitted polarization states

$$\epsilon_{in} = \frac{(|\mathbf{E}_\omega^+|^2 - |\mathbf{E}_\omega^-|^2)_{z=0}}{(|\mathbf{E}_\omega^+|^2 + |\mathbf{E}_\omega^-|^2)_{z=0}}, \qquad \epsilon_{tr} = \frac{(|\mathbf{E}_\omega^+|^2 - |\mathbf{E}_\omega^-|^2)_{z=L}}{(|\mathbf{E}_\omega^+|^2 + |\mathbf{E}_\omega^-|^2)_{z=L}}.$$

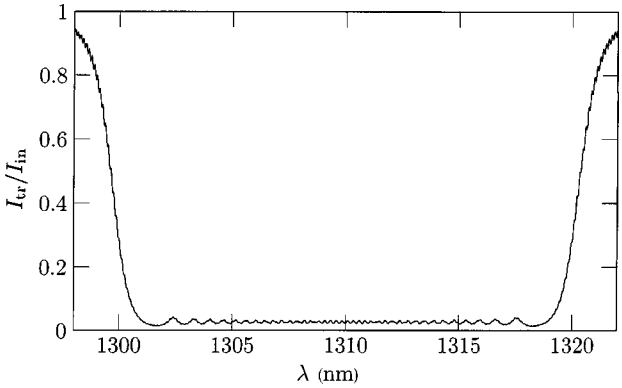

Fig. 3. Transmission spectrum of a linearly chirped, nonperturbed optical Bragg grating, in the absence of static magnetic fields. Parameters are the refractive-index bias $n_0 = 1.7$, the refractive-index modulation $n_1 = 2.5 \times 10^{-3}$, chirp $\xi = 1.47 \times 10^{-6}$, and initial grating period $\Lambda = 382.4\,\text{nm}$.

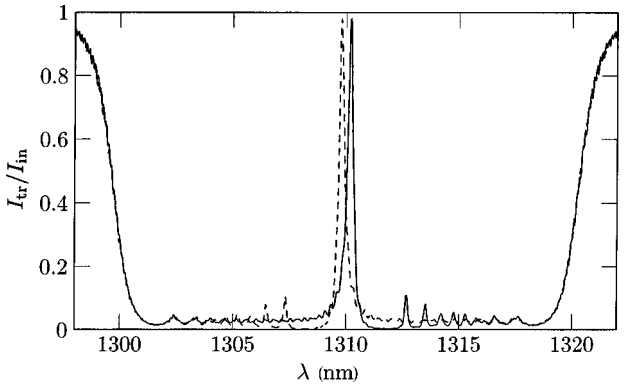

Fig. 4. Transmission spectrum of the linearly chirped grating of Fig. 3, with the magneto-optically induced gyration constant $g(z)$ as a superimposed Lorenzian perturbation, for left and right circularly polarized light (drawn as solid and dashed curves, respectively). Parameters used for the perturbation are $g_p = 5.0 \times 10^{-3}$ (amplitude), $w_p = 75$ μm (spatial half maximum width), and $z_p = 2.0$ mm (center position).

The normalized ellipticities take values between $\epsilon_{tr} = -1$ for right circularly polarized light and $\epsilon_{tr} = 1$ for left circularly polarized light with $\epsilon_{tr} = 0$ corresponding to linear polarization.

4. DEPENDENCE ON PERTURBATION STRENGTH

To illustrate the impact of the magneto-optically introduced perturbation upon the transmission characteristics, we consider the case of a single Lorentzian perturbation centered at the middle of the grating at $z_p = 2.0$ mm. For a perturbation peak value of $g_p = 5.0 \times 10^{-3}$ and a perturbation width of $w_p = 75$ μm, a transmission window is opened up in the middle of the blocking band of the chirped grating, as illustrated in Fig. 4. Since the magneto-optically induced perturbation $g(z)$ is added to the refractive-index profile with a different sign for orthogonal circularly polarized states, the peak transmission for those modes will be slightly shifted in the opposite directions of the center wavelength.

Whether one wishes to see the splitting of the transmission peak as a wanted or unwanted feature of the perturbation is a matter of application. For applications in which one wishes to resolve the two orthogonal circular polarization states with high precision, a linearly polarized input will yield the required sensitivity in the ellipticity of the transmitted polarization state in the spectral vicinity of the peak transmission. On the other hand, for applications in which one wishes only to transmit a single peak of a predetermined polarization state, a pure circularly polarized input is the proper choice, since no peak splitting of the transmission occurs for this case.

The physical explanation for the opening of the narrow transmission window is that when the perturbation $g(z)$ is applied to the bias of the refractive index, the original local resonance wavelength $\lambda_{loc}(z_p)$ at the perturbation center is shifted slightly to the resonance $\lambda_{loc}'(z_p) = [1 \pm (g_p/n_0)]\lambda_{loc}(z_p)$, with the positive/negative signs corresponding to left/right circular polarization. This shift will reduce the effective grating strength in the vicinity of the perturbation center z_p, instead increasing the grating strength in domains to the positive/negative side of the center z_p. This can be seen in Fig. 4, where the spectral domain just to the right of the center peak for left circular polarization (solid curve) has a slight suppression of the transmission, whereas the right circularly polarized mode instead has the suppression on the opposite side of the peak. Noteworthy is that contrary to such shifts induced by thermal or mechanical means, the current approach will shift the resonances to opposite directions in the spectrum.

In contrast to the case of a uniform, constantly distributed Faraday effect, the locally introduced perturbation $g(z)$ affects only the part of the spectrum that corresponds to the spatial neighboring domain of the perturbation. As can be seen in Fig. 4, the edges of the main window of the spectrum are left virtually unaffected by the perturbation, and no polarization state selectivity appears outside the region of the transmission peaks.

The transmission peak amplitude and position are dependent on the width and the amplitude of the introduced perturbation. In Fig. 5, a selected part of the spectrum of Fig. 4 is shown for right circularly polarized incident light, for perturbation widths of $w_p = 25$, 50, 75, and 100 μm. As shown in this figure, a perturbation width of 25 μm is not sufficient to cover a wide-enough part of the chirped grating to open a distinct transmission window, whereas one with a width of 100 μm has passed the optimum, slightly reducing the peak transmission. When the perturbation width is increased, the position of the peak transmission also drifts slightly. The FWHM of the peaks changes only marginally with the perturbation width; this is because the surrounding reflectance of the neighboring nonperturbed parts of the grating is essentially unchanged by the locally applied field, hence it still acts to efficiently cut the transmission outside the resonant region. The transmission window shapes corresponding to left circular polarization are shown in Fig. 6.

In connection with the peak separation between left and right circular polarization states, we also analyzed the spectral dependence of the polarization-state filtering of the device. Assuming a linearly polarized input beam, we expect from Fig. 4 that the spectral domain immediately to the left or right of the median center of the peaks

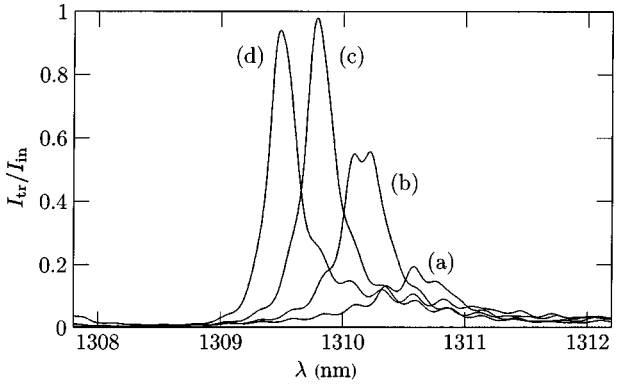

Fig. 5. Transmission window shape for a set of perturbation widths, shown for right circularly polarized light. The perturbation widths w_p used were, respectively, (a) 25 μm, (b) 50 μm, (c) 75 μm, and (d) 100 μm.

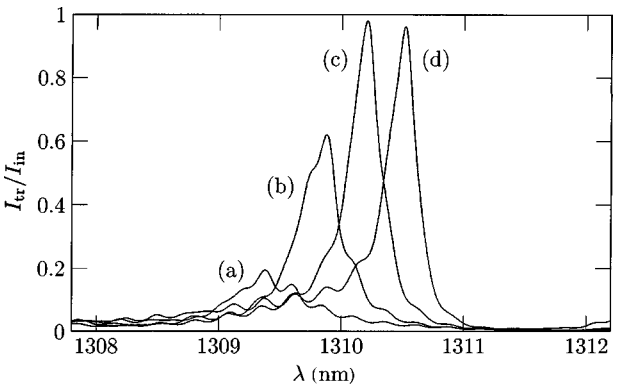

Fig. 6. Transmission window shape for a set of perturbation widths, shown for left circularly polarized light. The perturbation widths with respective labels are identical to those of the curves in Fig. 5.

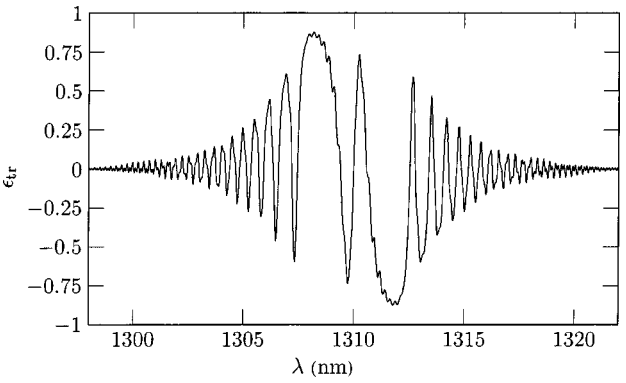

Fig. 7. Normalized ellipticity ϵ_{tr} of the transmitted polarization state as function of vacuum wavelength λ, for a linearly polarized input beam. The parameters used are identical to those used to generate the curves in Fig. 3.

would be highly transmitting for right or left circular polarization states. Figure 7 shows that this is also the case, with two distinct peaks switching between orthogonal circular polarization states close to a vacuum wavelength of 1310 nm. It is noteworthy that owing to the previously described suppression of transmission in the neighborhood of the peaks, we also have a comparatively broadbanded reversed ellipticity in the spectral regions surrounding $\lambda = 1308\,\text{nm}$ and $\lambda = 1312\,\text{nm}$. For these domains, however, one should keep in mind that the transmission is low, regardless of the polarization state, and that for most practical applications only the two centermost peaks are of interest.

5. TUNABILITY

We will now discuss the issue of the tunability of the proposed device. Since the periodicity of the grating is changing adiabatically with the spatial coordinate z, and since the shift of the resonance peaks is proportional to the peak amplitude of the introduced perturbation to the bias refractive index, one would expect the width and the peak transmission of the opened transmission peaks to be virtually constant under translation of the center of the perturbation, with only the spectral position of the peaks changing. For a real-world device, this change of position could, for example, be achieved through a mechanical translation of a current carrying wire along the z axis; or with transverse mesh of strip lines on a substrate, in a configuration similar to that shown in Fig. 1, where the current in each strip line could be controlled individually by an external current supply.

Figure 8 shows that the transmission peak actually is left virtually invariant in shape and amplitude under translation of the center of the perturbation; the same parameters as for the graph shown for left circular polarization in Fig. 4 were used, albeit now with a varying position z_p for the perturbation center. The perturbation width and amplitude were kept constant in the simulations.

Since multiple, spatially separated perturbations can easily be superimposed on the same chirped grating, the described principle of tuning can also be applied to the creation of a device operating as an optical interleaver, allowing one to selectively pick out a grid of discrete wavelengths in the spectrum. Such a device could typically be implemented in the design, as shown in Fig. 1, although with the S-shaped coil replaced by a transverse grid of strip lines, each one carrying a current in the same direction as the other strip lines.

6. CONCLUSIONS

For this analysis, we have considered the chirped grating to be generated by all-optical means. However, it should be emphasized that it equally may be an effective index grating generated by magneto-optical means, as illustrated in Fig. 1. To summarize the device proposed in this paper, we have shown the possibility of introducing magneto-optically induced perturbations in chirped optical Bragg gratings for opening up narrow transmission peaks in an otherwise-flat transmission blocking window. The impact of a varying spatial extent of the perturbation has been analyzed, and a physical explanation for the differential shift of the magneto-optically induced transmission peaks for left and right circular polarization states has been presented.

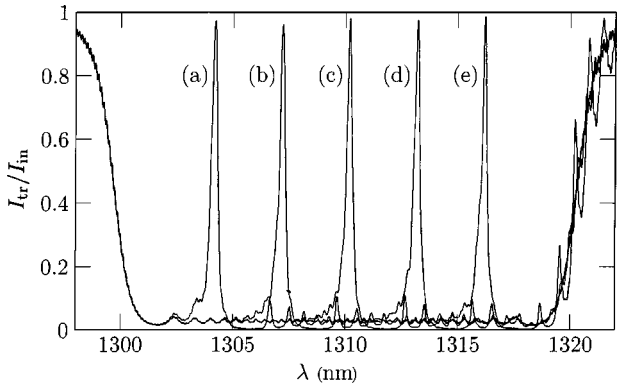

Fig. 8. Relative intensity transmission I_{tr}/I_{in} as function of vacuum wavelength λ, for a left circularly polarized incident beam, and for a magneto-optical perturbation with amplitude $g_p = 5.0 \times 10^{-3}$, width $w_p = 75\ \mu\text{m}$, at center positions (a) $z_p = 0.8\,\text{mm}$, (b) $z_p = 1.4\,\text{mm}$, (c) $z_p = 2.0\,\text{mm}$, (d) $z_p = 2.6\,\text{mm}$, and (e) $z_p = 3.2\,\text{mm}$. All other grating parameters are identical to those used for the graph in Fig. 4.

The novelty of the device as here proposed is the possibility of magneto-optically tailoring a narrow transmission window in an optically or magneto-optically induced, chirped-index grating, and also in that the resonance peak strength and position can be tuned by means of controlling the current carried by a transverse strip line and its spatial position along the grating.

REFERENCES

1. F. Jonsson and C. Flytzanis, "Polarization state controlled multistability of a nonlinear magneto-optic cavity," Phys. Rev. Lett. **82**, 1426–1429 (1999).
2. S. Wabnitz, E. Westin, R. Frey, and C. Flytzanis, "Soliton mode locking by nonlinear Faraday rotation," J. Opt. Soc. Am. B **13**, 2420–2423 (1996).
3. J. Fujita, M. Levy, R. Scarmozzino, R. M. Osgood, L. Eldada, and J. Yardley, "Integrated multistack waveguide polarizer," IEEE Photonics Technol. Lett. **10**, 93–95 (1998).
4. J. Fujita, M. Levy, R. M. Osgood, Jr., L. Wilkens, and H. Dötsch, "Waveguide optical isolator based on Mach–Zehnder interferometer," Appl. Phys. Lett. **76**, 2158–2160 (2000).
5. H. Kato and M. Inoue, "Reflection-mode operation of 1-dimensional magnetophotonic crystals for use in film-based magneto-optical isolator devices," J. Appl. Phys. **91**, 7017–7019 (2002).
6. W. Suh, M. F. Yanik, O. Solgaard, and S. Fan, "Displacement-sensitive photonic crystal structures based on guided resonance in photonic crystal slabs," Appl. Phys. Lett. **82**, 1999–2001 (2003).
7. R. Khomeriki and L. Tkeshelashvili, "Stable magnetostatic solitons in yttrium iron garnet film waveguides for tilted in-plane magnetic fields," Phys. Rev. B **65**, 134415 (2002).
8. F. J. Rachford, M. Levy, R. M. Osgood, Jr., A. Kumar, and H. Bakhru, "Magnetization and ferromagnetic resonance studies in implanted and crystal ion sliced bismuth-substituted yttrium iron garnet films," J. Appl. Phys. **85**, 5217–5219 (1999).
9. F. J. Rachford, M. Levy, R. M. Osgood, Jr., A. Kumar, and H. Bakhru, "Magnetization and FMR studies of crystal-ion-sliced narrow linewidth gallium-doped yttrium iron garnet," J. Appl. Phys. **87**, 6253–6255 (2000).
10. M. J. Steel, M. Levy, and J. R. M. Osgood, "Large magnetooptical Kerr rotation with high reflectivity from photonic bandgap structures with defects," J. Lightwave Technol. **18**, 1289–1296 (2000).
11. M. J. Steel, M. Levy, and J. R. M. Osgood, "Photonic bandgaps with defects and the enhancement of Faraday rotation," J. Lightwave Technol. **18**, 1297–1308 (2000).
12. M. J. Steel, M. Levy, and J. R. M. Osgood, "High transmission enhanced Faraday rotation in one-dimensional photonic crystals with defects," IEEE Photonics Technol. Lett. **12**, 1171–1173 (2002).
13. J. Su and C. S. Tsai, "Nonlinear characteristics of magnetooptic Bragg diffraction in bismuth substituted yttrium iron garnet films," J. Appl. Phys. **87**, 1474–1481 (2000).
14. C. Xu, X. Hu, Y. Li, X. Liu, R. Fu, and J. Zi, "Semiconductor-based tunable photonic crystals by means of an external magnetic field," Phys. Rev. B **68**, 193201 (2003).
15. J. L. Arce-Diego, R. López-Ruisánchez, J. M. López-Higuera, and M. A. Muriel, "Fiber Bragg grating as an optical filter tuned by a magnetic field," Opt. Lett. **22**, 603–605 (1997).
16. A. Othonos and K. Kalli, *Fiber Bragg Gratings* (Artech House, Norwood, Mass., 1999).
17. S. Jin, H. Mavoori, R. P. Espindola, and T. A. Strasser, "Broad-range, latchable reconfiguration of Bragg wavelength in optical gratings," Appl. Phys. Lett. **74**, 2259–2261 (1999).
18. J. Mora, B. Ortega, M. V. Andrés, J. Capmany, D. Pastor, J. L. Cruz, and S. Sales, "Tunable chirped fibre Bragg grating device controlled by variable magnetic fields," Electron. Lett. **38**, 118–119 (2002).
19. F. Jonsson and C. Flytzanis, "Optical amplitude and phase evolution in nonlinear magneto-optical Bragg gratings," J. Nonlinear Opt. Phys. Mater. **13**, 129–154 (2004).
20. S. Kielich and R. Zawodny, "Optical nonlinear phenomena in magnetized crystals and isotropic bodies," Acta Phys. Pol. A **43**, 579–602 (1973).
21. L. D. Landau, E. M. Lifshitz, and L. P. Pitaevskiĭ, *Electrodynamics of Continuous Media*, 2nd ed. (Butterworth–Heinemann, Stoneham, Mass., 1984).
22. R. Feced, M. N. Zervas, and M. A. Muriel, "An efficient inverse scattering algorithm for the design of nonuniform fiber Bragg gratings," IEEE J. Quantum Electron. **35**, 1105–1115 (1999).